PNAS Nexus, 2022, 2, 1–5
https://doi.org/10.1093/pnasnexus/pgac307
Advance access publication date: 24 December 2022
Brief Report

Three-dimensional coordination of cell-division site positioning in a filamentous cyanobacterium

Jing Liu[a,b,1], Wei-Yue Xing[a,1], Bowen Liu[c] and Cheng-Cai Zhang[a,c,d,*]

[a]State Key Laboratory of Freshwater Ecology and Biotechnology and Key Laboratory of Algal Biology, Institute of Hydrobiology, Chinese Academy of Sciences, Wuhan, Hubei 430072, People's Republic of China
[b]University of Chinese Academy of Sciences, Beijing 100049, People's Republic of China
[c]Institut WUT-AMU, Aix-Marseille Université and Wuhan University of Technology, Wuhan, Hubei 430070, People's Republic of China
[d]Innovation Academy for Seed Design, Chinese Academy of Sciences, Beijing 100049, China
*To whom correspondence should be addressed. Email: cczhang@ihb.ac.cn
[1]the two authors contributed equally to this work.
Classification: Major, Biological Sciences. Minor, Microbiology.
Edited By: Christopher Dupont

Abstract

Bacterial cells mostly divide symmetrically. In the filamentous, multicellular cyanobacterium *Anabaena*, cell-division planes are aligned vertically relative to the long axis of every single cell. This observation suggests that both the placement and the angle of the division planes are controlled in every single cell so that the filament can grow in one single dimension along the long axis. In this study, we showed that inactivation of *patU3* encoding a cell-division inhibitor led cells to divide asymmetrically in two dimensions leading to twisted filaments, indicating that PatU3 controls not only the position but also the angle of the division planes. Deletion of the conserved *minC* and *minD* genes affected cell division symmetry, but not the angle of the division planes. Remarkably, when both *patU3* and *minCD* were inactivated, cells could divide asymmetrically over 360° angles in three dimensions across different cellular sections, producing not only cells with irregular sizes, but also branching filaments. This study demonstrated the existence of a system operating in a three-dimensional manner for the control of cell division in *Anabaena*. Such a regulation may have been evolved to accommodate multicellular behaviors, a hallmark in evolution.

Keywords: cell division, division symmetry, cyanobacteria, DNA segregation, multicellularity

Significance Statement:

Most of our knowledge about cell division control has been generated by using rode-shaped unicellular bacteria such as *Escherichia coli* and *Bacillus subtilis*. Our studies in the multicellular filamentous cyanobacterium *Anabaena* reveal not only the function of the conserved Min system for cell-division site selection, but also a protein conserved in filamentous cyanobacteria for the placement of cell-division site at the right place in a right angle. These regulation systems link cell division to filament morphology at a multicellular level, and will help us to understand the morphological diversification of cyanobacteria during evolution.

Introduction

Most bacteria divide by binary fission, leading to two daughter cells of equal size. In *Escherichia coli*, symmetric cell division and the timing of septation during the cell cycle are achieved by the regulatory system Min composed of MinC, MinD, and MinE, and the nucleoid occlusion system involving SlmA (1, 2). MinC inhibits cell division by promoting the depolymerization of FtsZ (3). MinD, as a carrier for MinC, is associated to the inner cytoplasmic membrane and oscillates from one cell pole to another in a MinE-dependent manner (4). *Anabaena* PCC 7120 (*Anabaena*) is a multicellular organism with intercellular exchange of nutrients and signals for filament growth and environmental adaptation (5). *Anabaena* cells divide symmetrically, with the division planes of different cells placed in parallel, in a 90° angle relative to the long axis of the filaments (6). This one-dimensional division mode not only guarantees cell division symmetry, but also the morphology of the filament that grows in one dimension.

Results

Previously, we showed that PatU3, when accumulated, acted as a cell division inhibitor in *Anabaena* (7), but the phenotype of Δ*patU3* was poorly characterized. We showed here that Δ*patU3* displayed many dividing cells generating two daughter cells of unequal size (Fig. 1A), suggesting the occurrence of asymmetric cell division. To study the control of cell division site positioning, we also created a Δ*minCD* mutant with deletion of *minC* and *minD*, and a double mutant Δ*minCD*Δ*patU3*. We then examined cell-division

Competing interest : The authors declare no competing interests.
Received: September 28, 2022. **Accepted:** December 23, 2022

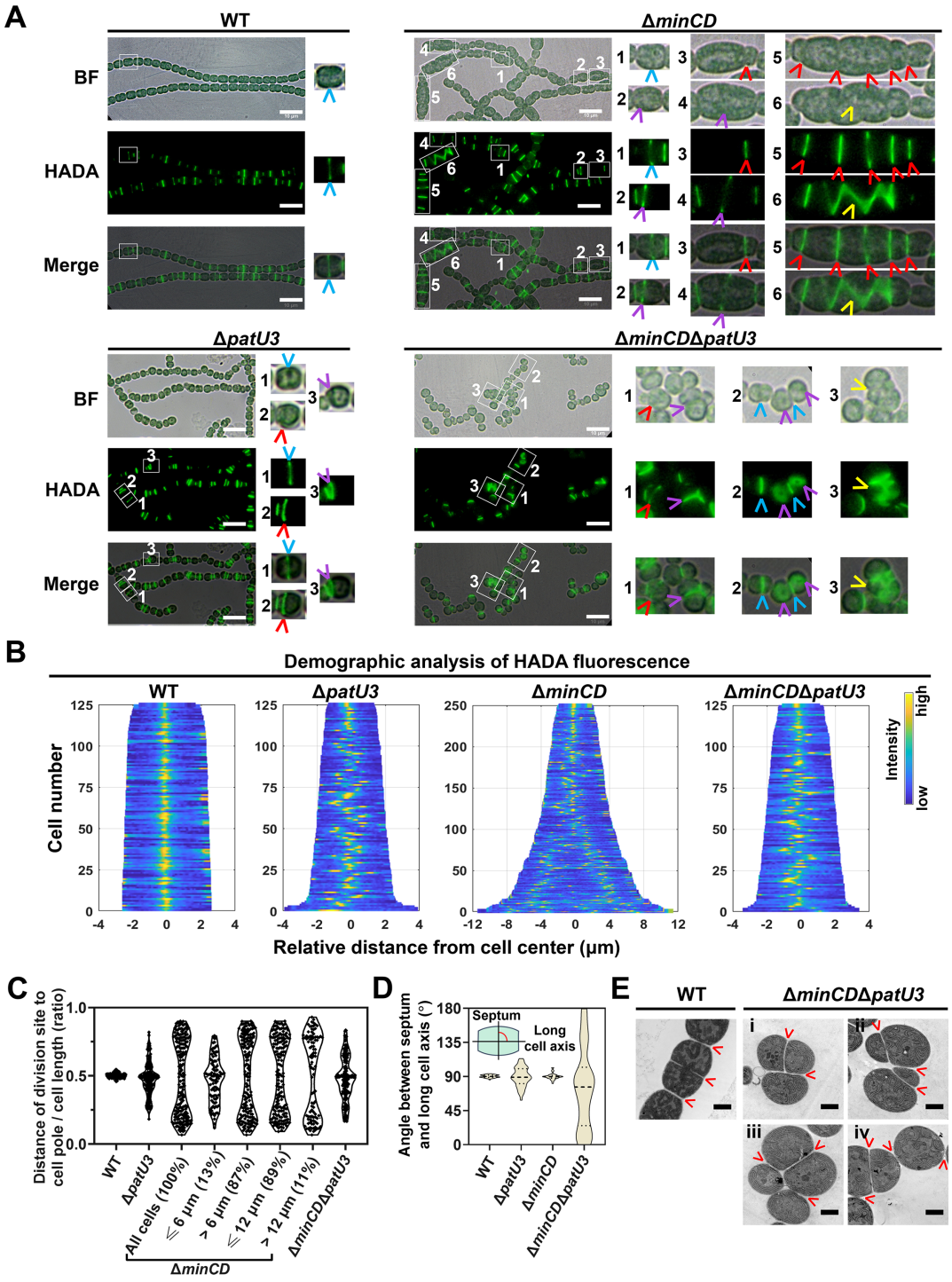

Fig. 1. Synthetic effects of *patU3* and *minCD* on the placement of cell division sites. (A) Cell division planes were labeled with HADA fluorescence. Zoomed-in parts display examples of symmetric cell division (blue arrows), asymmetric cell division (red arrows), or tilted division planes (purple arrows). Yellow arrows indicate a spiral division plane. Scale bar: 10 μm. (B) Demographic analysis showing the fluorescence intensity profile of HADA along the cell length in a cell population of different strains. (C) Relative positions of cell division sites based on HADA labeling. $n = 200$ cells, except for 100 cells were analyzed in cells shorter than 6 μm (13%) or longer than 12 μm (11%) of Δ*minCD*. (D) Analysis of the angles of the division planes in dividing cells following HADA fluorescence labeling. n = 50 dividing cells. (E) Micrographs of WT and Δ*minCD*Δ*patU3* obtained by transmission electron microscopy (TEM). Red arrows indicate the septa of cells. Scale bar in black: 1 μm.

patterns following septal labeling by 7-hydroxycoumarin-amino-D-alanine (HADA) (8, 9). Asymmetric cell division was found to occur in all three mutants (Figs. 1A and B). Although all mutants showed cell size heterogeneity in comparison to the WT, the strongest effect was observed for Δ*minCD* in which giant cells with two polar division sites or what appeared to be a spiral division plane across the whole cell were observed (Figs. 1A and B). HADA labeling was found mainly between 0.4 and 0.6 (0 and 1 representing the two cell poles and 0.5 the center) of the relative cell lengths in Δ*patU3*, thus in proximity to the midcell position; only a small proportion of HADA labeling (13.3%) occurred similarly as in the WT (Fig. 1C). By comparison, asym-

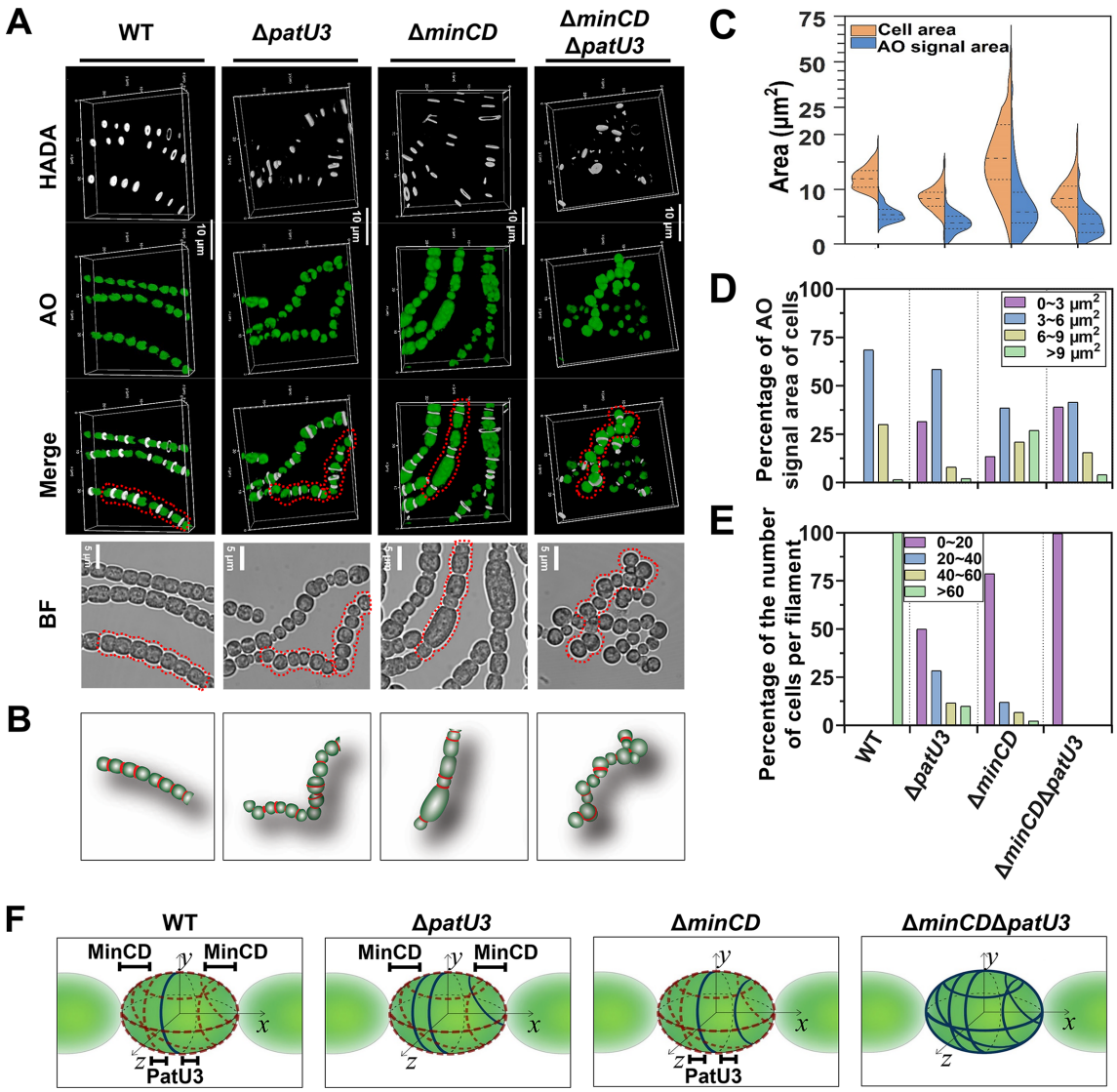

Fig. 2. Three-dimensional control of division site positioning in *Anabaena*. (A) Confocal microscopic images of different strains after staining with HADA for septa (white color) and AO for nucleoid DNA (green color). The size was indicated by scale bars. (B) Schematic drawing of representative filaments from panel A rounded up by dotted red line. Solid red lines represent division planes. (C) Analysis of cell area and AO signal area of cells. $N = 200$ cells. (D) Graphs showing the percentage of AO signal area in different strains based on the data shown in panel C. (E) Bar graphs showing the percentage of filament length (number of cells per filament) distribution of different strains. $n = 250$ filaments. (F) Proposed model for three-dimensional control of cell division site placement by PatU3 and Min in *Anabaena*. x, y, and z, the three dimensions of a cell. Dotted red lines represent potential cell division sites, yet repressed (black bars above the cell) by the Min system at the polar sites or PatU3 at sites close to the cell center. Blue lines represent one of the potential division planes that may occur in a cell division process.

metric labeling of HADA was found mostly towards the polar regions, around 0.2 and 0.8 of the relative cell length in Δ*minCD*, relatively away from cell centers. Since Δ*minCD* presented a high cell size heterogeneity, we separated the cell population according to cell lengths for a more detailed analysis (Fig. 1C). For cells shorter than 6 μm, the pattern of septal positioning was similar to Δ*patU3*. In contrast, for cells longer than 6 μm, most cell division sites occurred at polar regions, consistent with demographic analysis (Fig. 1B). The double mutant Δ*minCD*Δ*patU3* displayed a phenotype in cell division asymmetry that appeared weaker than that in Δ*minCD*, and stronger than that of Δ*patU3* (Figs. 1B and C). In fact, as described below, the phenotype was the strongest in the double mutant, but the quantification of the polar division pattern shown in Fig. 1C was made difficult because of the highly twisted filaments formed in the double mutant.

In addition to cell division asymmetry, division planes marked by HADA labeling were tilted in some mutant cells, instead of being vertically aligned in a 90° angle relative to the long filament axis as in the WT (Fig. 1D). In Δ*patU3*, the angle of the septa was in the range of 60°–120°, and only 36% of the angles were vertical (Fig. 1D). These results could explain the irregularity of cell size, as well as the occurrence of twisted filaments in Δ*patU3*, caused by changes in the angle of the division planes. In Δ*minCD*, almost all cell division planes were still placed in a 90° angle relative to the long cell axis. In Δ*minCD*Δ*patU3*, a striking disorder of cell division angle was observed, while in some extreme cases, horizontal cell division could occur (0° or 180° relative to the long cell axis), leading to branching of the filament (Fig. 1D). The deviation by up to 180° could occur on either side of the long filament axis, which indicated that cell division could take place at any angle, in the range of 360°. For example (number 2, Fig. 1A), on both sides of

a horizontally positioned division plane, one vertically positioned division plane could be seen. This branching effect led to network-like filaments, ramifying in three dimensions instead of the one-dimensional growth observed in the WT filaments.

To confirm the branching of the highly distorted filaments in Δ*minCD*Δ*patU3*, we used TEM to observe septa positioning and filament morphology (Fig. 1E). Compared to symmetric and vertical division planes in WT cells, Δ*minCD*Δ*patU3* cells could divide with different angles along any of the cell or filament axes (Fig. 1E), or in a polar region (image ii, Fig. 1E). Confocal microscopic data (Fig. 2A; Supplementary Material Videos) with HADA (late stage of septa) and acridine orange (AO) (nucleoids) staining (8, 10), helped by schematic drawing of representative images (Fig. 2B), allowed us to visualize the distortion of the filament as a consequence of tilted division planes in Δ*patU3*, polar division sites placed in parallel in cells of Δ*minCD*, and branching filaments in Δ*minCD*Δ*patU3* as a result of cell division occurring at multiple possible orientations. As shown by AO straining, asymmetric cell division strongly affected DNA segregation (Fig. 2C), with extreme cases in which DNA-less minicells could be found, and could cause cell death and filaments breakage (Fig. 2D and E).

Discussion

In most mutants affecting cell division in rod-shaped bacteria such as *E. coli* or *B. subtilis*, cell division planes are still placed vertically along the long cell axis. In some cells of the Δ*zapA* and Δ*zapB* mutants, or some alleles of *ftsZ* in *E. coli*, a tilted Z ring has been noticed (11, 12). In the spherical cell-shaped bacterium *Staphylococcus aureus*, cell division planes are placed at multiple angles over the generations (13). Similar effects could also be observed in cells of the *E. coli rodA* Δ*min* mutant converted to a spherical shape (14). In this study, we revealed the existence of a three-dimensional control system of cell division in *Anabaena* forming multicellular filaments. As illustrated by the schematic drawing in Fig. 2F, in WT and Δ*minCD*, cell division occurs in a one-dimensional manner, vertically along the long filament axis (axis *x*). In the *patU3*-deficient mutant, cell division may occur in two dimensions in an angle ranging from 60 to 120°, representing the short and the long cell axis of a filament (axis *x, y*). When both the Min system and PatU3 are absent, cell division may occur in three dimensions at all possible angles (0–360°) and across different cell sections (axis *x*, *y*, and *z*), with branching of the filaments. Based on these results, we propose that both the Min system and PatU3 inhibit alternative division sites at the polar regions of a cell, with PatU3 acting in subregions closer to the cell center, while MinCD closer to the cell poles (Fig. 2F). In addition, PatU3 restricts the angle of the division planes to 90° relative to the long cell axis, all in parallel in different cells, producing straight filament. Some cyanobacteria grow with naturally branching filaments (15). However, PatU3, or its longer version PatU, exists in all sequenced filamentous cyanobacteria, with or without branching. It would be interesting to investigate whether the expression or subcellular localization of PatU3, could be involved in the branching process (15). The mechanism for the function of PatU3 also remains to be determined. PatU3 could coalesce the Z-rings to better orientate the division site. Alternatively, it could play a role in a nucleoid occulsion system, which could be consistent with its effects observed at subcellular regions closer to the cell center.

Our studies revealed a regulation system for the positioning of division sites in *Anabaena*, with PatU3 as a unique component of the system conserved in filamentous cyanobacteria. The results reported here paved the way for our understanding on cyanobacterial cell division control, which operates in a three-dimensional manner. The appearance of multicellular behaviors is a hallmark in biological evolution, and such a coordination system may have been evolved in order to maintain filament morphology by controlling the positioning of division planes among different cells of a multicellular filament.

Supplementary Material

Supplementary Material is available at *PNAS Nexus* online.

Funding

This work was supported by the National Natural Science Foundation of China [Grant No. 92051106, and Youth Program Grant No. 31800033 and 32200028], and the Featured Institute Service Projects from the Institute of Hydrobiology [Grant No. Y85Z061601].

Authors' Contributions

J.L., W.Y.X., and B.L. performed the experiments. C.C.Z., J.L., and W.Y.X. designed experiments. C.C.Z. and L.J. wrote the manuscript.

Data Availability

All data are included in the manuscript and/or supporting information.

References

1. De Boer PA, Crossley RE, Rothfield LI. 1989. A division inhibitor and a topological specificity factor coded for by the minicell locus determine proper placement of the division septum in *E. coli*.Cell. 56:641–649.
2. Lutkenhaus J. 2007. Assembly dynamics of the bacterial MinCDE system and spatial regulation of the Z ring. Annu Rev Biochem. 76:539–562.
3. Hu Z *et al.* 1999. The MinC component of the division site selection system in *E. coli* interacts with FtsZ to prevent polymerization. Proc Natl Acad Sci USA. 96:14819–14824.
4. Park KT *et al.* 2017. MinE conformational dynamics regulate membrane binding, MinD interaction, and Min oscillation. Proc Natl Acad Sci USA. 114:7497–7504.
5. Zeng X, Zhang CC. 2022. The making of a Heterocyst in Cyanobacteria. Annu Rev Microbiol. 76:597–618, doi.org/10.1146/annurev-micro-041320-093442, in press.
6. Sakr S *et al.* 2006. Inhibition of cell division suppresses heterocyst development in *Anabaena* sp. strain PCC 7120. J Bacteriol. 188:1396–1404.
7. Xing WY *et al.* 2022. A proteolytic pathway coordinates cell division and heterocyst differentiation in the cyanobacterium *Anabaena* sp. PCC 7120. Proc Natl Acad Sci USA. 119:e2207963119.
8. Kuru E *et al.* 2015. Synthesis of fluorescent d-amino acids and their use for probing peptidoglycan synthesis and bacterial growth in situ. Nat Protoc. 10:33–52.
9. Xing WY *et al.* 2021. HetF protein is a new divisome component in a filamentous and developmental cyanobacterium. mBio. 12:e0138221.
10. Canini A, Caiola MG, Ferrucci L. 1992. Quantitative and qualitative DNA variations in *Anabaena azollae* strasb. living in *Azolla filiculoides* lam. Cytometry.13:299–306.

11. Buss J *et al.* 2013. *In vivo* organization of the FtsZ-ring by ZapA and ZapB revealed by quantitative super-resolution microscopy. Mol Microbiol.89:1099–1120.
12. Bi E, Lutkenhaus J. 1992. Isolation and characterization of *ftsZ* alleles that affect septal morphology. J Bacteriol. 174:5414–5423.
13. Saraiva BM *et al.* 2020. Reassessment of the distinctive geometry of *Staphylococcus aureus* cell division. Nat Commun. 11:4097.
14. Corbin BD, Yu XC, Margolin W. 2002. Exploring intracellular space function of the min system in round-shaped *E. coli*. EMBO J.21:1998–2008.
15. Nürnberg DJ *et al.* 2014. Branching and intercellular communication in the section V cyanobacterium *Mastigocladus laminosus*, a complex multicellular prokaryote. Mol Microbiol. 91: 935–949.